

LATERAL GROWTH RATES IN LASER CVD OF TUNGSTEN MICROSTRUCTURES

T. SZÖRÉNYI, K. PIGLMAYER, G.Q. ZHANG and D. BÄUERLE

Angewandte Physik, Johannes-Kepler-Universität Linz, Austria

Received 28 January 1988; accepted for publication 6 April 1988

The lateral growth rates observed during the Kr^+ laser-induced deposition of W spots from gaseous mixtures of WF_6 and H_2 have been analyzed on the basis of model calculations for pyrolytic laser-CVD. The apparent chemical activation energies derived for substrates of fused quartz (a-SiO_2) covered either with 700 Å of sputtered W or with 1200 Å of amorphous Si (a-Si) are 30 and 40 kcal/mol, respectively.

1. Introduction

Laser-induced chemical vapor deposition (LCVD) permits maskless single-step fabrication of thin films with lateral dimensions down into the submicrometer range [1,2]. While the technique has been demonstrated for a great variety of different materials, a detailed analysis of the experimental data has only been performed in a very few cases.

In this paper, we report on the laser-induced deposition of W spots by hydrogen reduction of WF_6 under 647.1 nm Kr^+ laser irradiation. Recent investigations on the laser-induced direct writing of W stripes using similar conditions have led us to speculate that the deposition process is photothermally (pyrolytically) activated [3]. This will be proved in the present paper by analyzing the lateral growth rates of laser-deposited W spots on the basis of model calculations for pyrolytic LCVD [1,4,5].

The paper is organized as follows. After a brief description of the experimental setup in section 2, the experimental results will be presented in section 3. In section 4 we outline the main features of the model calculations. The analysis of the experimental data is discussed in section 5.

2. Experimental

The experimental setup used in the present investigations was similar to that described in ref. [3]. The 647.1 nm TEM_{00} beam of a CW Kr^+ laser was

focused onto the substrate surface by a combination of a beam-expanding lens and a microscope objective. The position of the objective was optically and electronically controlled to keep the laser focus $2w_0$ (defined by the $1/e^2$ decrease in intensity) on the substrate surface constant (autofocus-system) at a value of $3 \mu\text{m}$. The incident laser power and laser beam illumination time (ranging from one millisecond up to several tens of seconds) was controlled by means of an acousto-optical modulator. The power meter was calibrated to the effective laser power incident onto the substrate surface. The whole system, including the xyz -translation of the reaction chamber, was controlled by means of a microcomputer. The substrates used were fused quartz plates (a-SiO_2 ; Suprasil I from Heraeus) covered either with 700 \AA of sputtered W or with 1200 \AA of sputtered amorphous Si (a-Si). The region of the substrate where deposition takes place was illuminated by a fiber optic source so that the growth of spots could be observed in situ by a microscope arrangement. The WF_6 gas used throughout the experiments was supplied by Fluka-Chemie. It has a purity of 99.56% with mainly tungsten oxyfluorides ($< 0.4\%$), CF_4 ($< 0.025\%$), HF ($< 0.01\%$), and SF_6 ($< 0.01\%$) as contaminants.

In the present investigations constant partial pressures of 5 mbar WF_6 and 500 mbar H_2 have been used. With the 700 \AA W/ a-SiO_2 substrate good reproducibility of data was obtained only when the partially oxidized W surface was reduced in H_2 atmosphere prior to the deposition process. The W reduction was performed either in an oven or by means of laser beam illumination directly within the reaction chamber.

3. Results

Figs. 1a–1h show scanning electron micrographs of W spots deposited onto a 700 \AA W/ a-SiO_2 substrate. The only parameter change in the deposition process was the laser beam illumination time t_i , which was increased for each successive spot. This time-dependent growth of spots is characterized by changes in both morphology and microstructure: with increasing laser beam illumination time t_i , the diameter d and the maximum height h of the spots increase, while the ratio of d and h decreases. The microstructure of the deposited W is polycrystalline. The grain size is very small with short illumination times, and increases with increasing t_i . For longer illumination times, the growth of one or several single crystals is observed (fig. 1h). When t_i is increased even further, the growth of a rod along the axis of the laser beam is observed [1,6,7]. For the 1200 \AA a-Si/a-SiO_2 substrate, there is a similar time evolution of the W spots. The only differences are: a slight deepening in the amorphous silicon layer near the rim of the spots, and a small dip in the center of spots which is observed for illumination times $t_i < 0.05$ s.

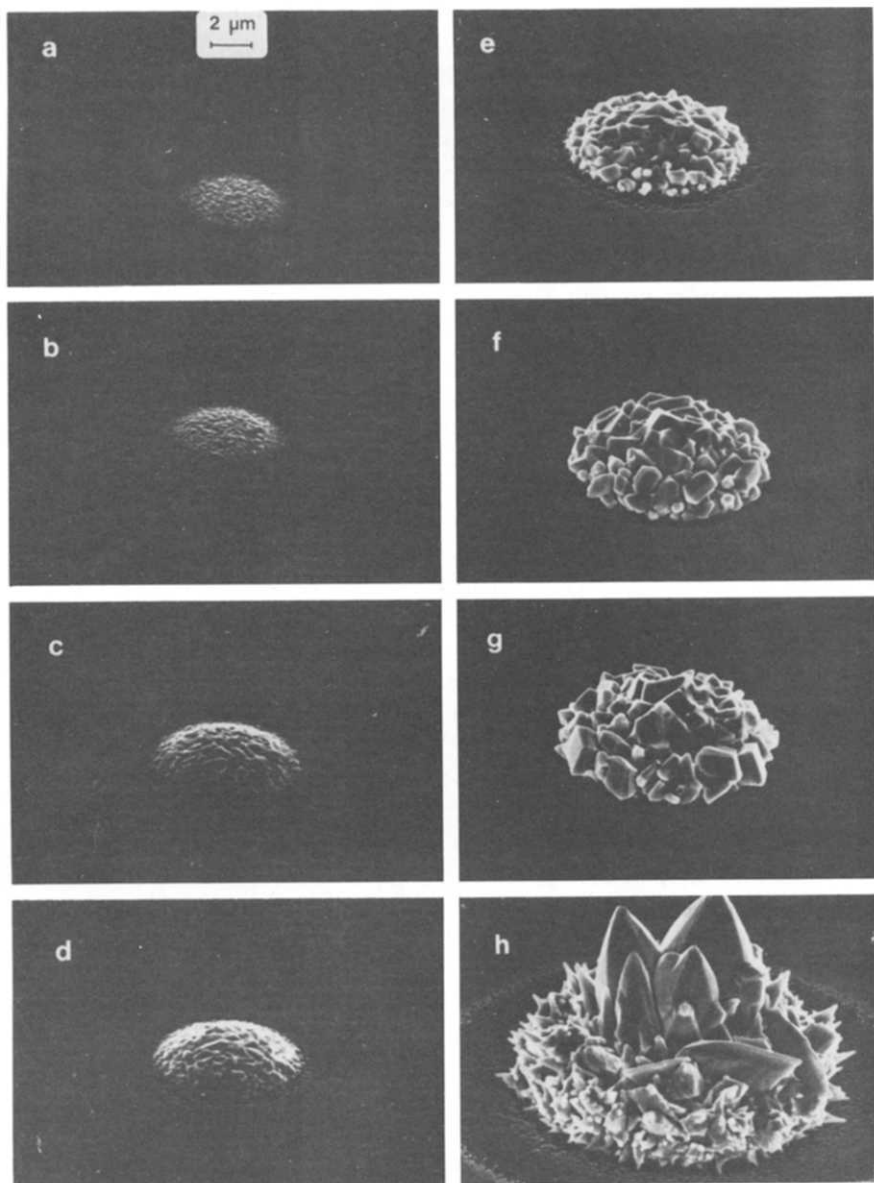


Fig. 1. W spots deposited from an admixture of 5 mbar WF_6 and 500 mbar H_2 by means of 647.1 nm Kr^+ laser radiation ($P=178$ mW, $2w_0=3.0$ μm). The substrate was fused quartz ($a\text{-SiO}_2$) covered with a 700 \AA thick layer of sputtered W. The laser beam illumination time t_l was increased successively from (a) to (h) as follows: (a) 0.01 s, (b) 0.02 s, (c) 0.05 s, (d) 0.07 s, (e) 0.1 s, (f) 0.2 s, (g) 0.3 s, (h) 0.5 s.

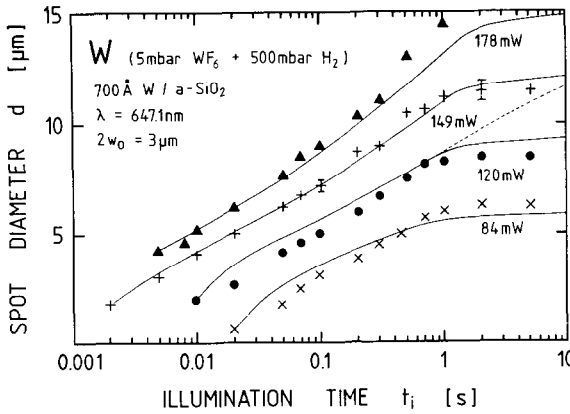


Fig. 2. Diameter of W spots for various laser powers as a function of 647.1 nm Kr⁺ laser beam illumination time. The laser focus was $2w_0 = 3.0 \mu\text{m}$. The partial pressures of gases were $p(\text{WF}_6) = 5 \text{ mbar}$ and $p(\text{H}_2) = 500 \text{ mbar}$. The substrate was a-SiO₂ covered with 700 Å sputtered W. The laser powers were: (x) 84 mW, (●) 120 mW, (+) 149 mW, (▲) 178 mW. Full and dashed curves have been calculated.

The diameter of W spots as a function of laser beam illumination time t_i is shown in figs. 2 and 3 for the two substrate materials and for various laser powers. Each data point has been derived from ten spots. The error bars represent the standard deviations, and are of similar sizes in the case of the other laser powers investigated in the respective regions of illumination times. The somewhat greater uncertainty of data points observed for the longer irradiation times originates from the inferior definition of the spot diameter in this regime (see fig. 1h). With both types of substrates employed, the spot

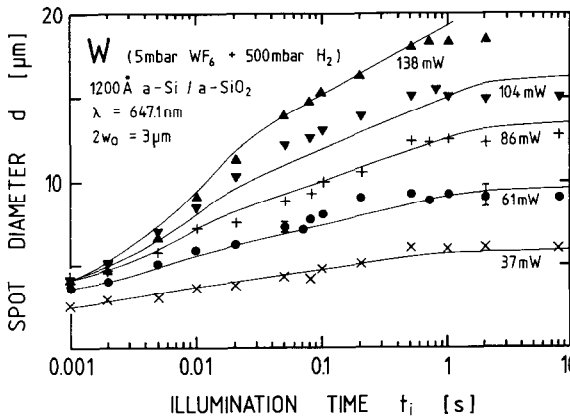


Fig. 3. Same as fig. 2 but with an 1200 Å a-Si/a-SiO₂ substrate. The laser powers were: (x) 37 mW, (●) 61 mW, (+) 86 mW, (▼) 104 mW, (▲) 138 mW.

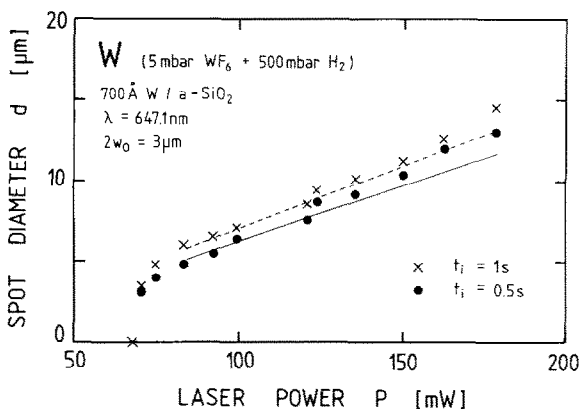


Fig. 4. Diameter of W spots as a function of laser power (647.1 nm Kr^+ , $2w_0 = 3.0 \mu\text{m}$) for two laser beam illumination times t_i . The substrate was 700 Å W/a-SiO₂. The partial pressures employed were $p(\text{WF}_6) = 5 \text{ mbar}$ and $p(\text{H}_2) = 500 \text{ mbar}$. The curves have been calculated.

diameters first increase very rapidly with t_i and then saturate at certain diameters d_{max} which depend on the laser power. With the a-Si/SiO₂ substrate (fig. 3), saturation occurs within somewhat shorter times and at diameters somewhat larger than with the W/SiO₂ substrate (fig. 2). It is remarkable that with the 700 Å W/a-SiO₂ substrate the spot sizes become considerably larger, depending on the thickness of the oxide layer formed, if the W surface is *not* reduced prior to deposition.

Fig. 4 shows the diameter of spots as a function of laser power for a 700 Å W/a-SiO₂ substrate and two times of laser beam illumination. Independently of t_i , deposition starts only above a threshold power of $60 \pm 1 \text{ mW}$. Above this threshold, the diameter of spots increases first very steeply and then continues to increase about linearly with laser power.

The quasi-linear increase in spot diameters observed in the semilogarithmic plots of figs. 2 and 3, and the linear plot of fig. 4, directly suggests a thermal activation of the deposition process [1]. We shall therefore attempt to analyze the experimental results on the basis of the model calculations for pyrolytic LCVD which are presented in the following section.

4. Model calculations

Reliable in-situ temperature measurements in laser chemical processing (LCP) are still only possible under quasistationary conditions such as, for example, the steady growth of rods [1,6]. During the deposition of spots, however, the laser-induced temperature distribution changes so rapidly with the laser beam illumination time t_i that it can only be evaluated from model

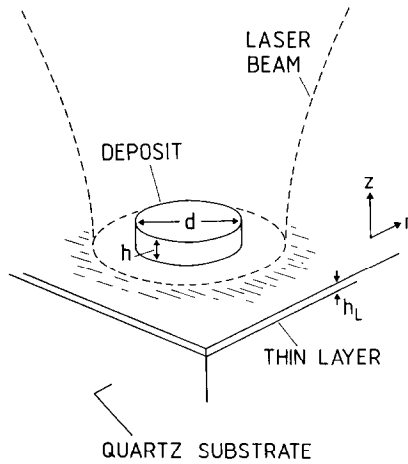


Fig. 5. Model structure of spots employed in the temperature calculations. The diameter of the deposit is d and its height is h . The thickness of the thin intermediate layer is h_L . The diameter of the laser spot on the substrate is $2w_0$.

calculations. A model structure that is appropriate to the present experimental situation is shown in fig. 5. The W spot is represented by a circular cylinder (height h , diameter d) with a thermal conductivity κ_D . Note that the exact shape of the model structure has only a minor influence on the laser-induced temperature distribution as long as temperature differences within the deposit are small compared to the maximum laser-induced temperature rise [4,5]. The thermal conductivities of the thin layer h_L and the quartz glass are henceforth denoted by κ_L and κ_S , respectively. In general, these quantities are temperature-dependent. Clearly, for tungsten the thermal conductivity is very large compared to that of quartz glass, i.e. $\kappa_D \gg \kappa_S$ for all laser powers investigated.

The laser-induced temperature distribution $T(r, z)$ for the model structure shown in fig. 5 can be calculated from the stationary heat equation

$$-\nabla(\kappa(T)\nabla T) = Q. \quad (1)$$

Here we have accounted for the fact that within the range of experimental parameters investigated no surface melting will occur (the melting temperature of W is $T_m(W) = 3663$ K). Q is the source term arising from the absorbed laser light and κ refers to κ_D , κ_L and κ_S . The assumption of stationary conditions is a good approximation because the velocity of propagation of the temperature profile which is approximately given by $v_t = dl/dt = (D_t/4t_i)^{1/2}$ is, for all of the laser beam irradiation times t_i investigated in the present experiments, very large compared to the observed growth rates of the W spots. In the worst case, i.e. with the a-Si/a-SiO₂ substrate ($D_t \approx 10^6 \mu\text{m}^2/\text{s}$) and with illumination times $t_i \approx 10^{-3}$ s, a simple estimation yields a value of $v_t \approx 1.6 \times 10^4$

$\mu\text{m/s}$, which is very large compared to the corresponding growth velocity of approximately $3 \times 10^2 \mu\text{m/s}$ (see below, fig. 8).

Because of the large range of laser powers investigated in the present experiments, consideration of the temperature dependencies of κ_D , κ_L and κ_S is required. For bulk tungsten, the temperature dependence of κ_D can be derived for the temperature range $300 \leq T \leq 2000$ K from data given in ref. [8], and it can be well described by

$$\kappa_D(W, T) = c_1 + c_2/T + c_3/T^2, \quad (2)$$

with $c_1 = 85.29 \text{ W/m K}$, $c_2 = 3.795 \times 10^4 \text{ W/m}$, and $c_3 = -2.996 \times 10^6 \text{ W K/m}$. The room temperature thermal conductivities of laser-deposited W films and of sputtered W layers have been estimated from the Wiedemann–Franz law by employing the electrical resistivities measured by means of a four-point probe technique; the respective values derived from these measurements were smaller and only 0.55 (see also ref. [3]) and 0.5 times the thermal conductivity of bulk tungsten. The thermal conductivities of the W spots and of the sputtered W layer inserted into the calculations were therefore corrected by these factors, while their temperature dependencies have been assumed to follow (2). For the fused quartz employed in our experiments, measurements on the temperature dependence of the thermal conductivity were available up to temperatures of $T \approx 1300$ K [9]. By fitting these experimental data we obtain

$$\kappa_S(\text{a-SiO}_2, T) = a_1 + a_2 T, \quad (3)$$

with $a_1 = 0.9094 \text{ W/m K}$ and $a_2 = 1.422 \times 10^{-3} \text{ W/m K}^2$. For the thermal conductivity of the amorphous Si layer we use the approximation $\kappa_L(\text{a-Si}) \approx \kappa_S(\text{a-SiO}_2)$ [10]. Furthermore, we extrapolate eqs. (2) and (3) up to the highest laser-induced temperatures of about $T \approx 2800$ K, as considered in the present experiments.

The reflectivity of the W that enters the source term in (1) has been assumed to be constant, which is a good approximation within the temperature regimes investigated in the present experiments [11]. For both the deposit and the thin sputtered W layer, we have used the reflectivity value measured for the W layer, which was $R(T = 300 \text{ K}) \approx 0.54 \pm 0.01$.

We now briefly describe the further assumptions and the results obtained with the two different substrate materials employed in the experiments:

(i) For the 1200 \AA a-Si/a-SiO₂ substrate we neglect any temperature gradients within the W deposit, which has been proved to be a good approximation in cases where $\kappa_D \gg \kappa_S$ [1,5]. In other words, the laser-induced temperature within the deposit is constant, i.e.

$$T(r, z) = T_\ell = \text{constant} \quad \text{for } r \leq d/2 \quad \text{and} \quad 0 \leq z \leq h, \quad (4)$$

where, in particular, T_ℓ is the temperature at the edge of the deposit on the substrate surface. With the approximations and assumptions made, eq. (1) can

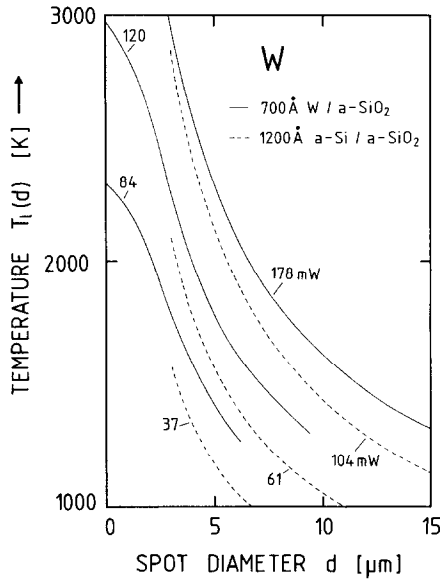


Fig. 6. Temperature at the edge of spots calculated as a function of spot diameter for the two substrate materials, and for laser powers employed in the experiments. The full curves refer to the 700 Å W/a-SiO₂ substrate (fig. 2) while the dashed curves refer to the 1200 Å a-Si/a-SiO₂ substrate (fig. 3).

be solved analytically by applying a Kirchhoff transform to a formalism proposed in ref. [12], as long as the diameter of W spots is larger than the diameter of the laser beam, i.e. if $d \geq 2w_0$. This latter condition is indeed fulfilled for all of the laser beam illumination times investigated in the experiments (see fig. 3). The temperature T_e can then be described by

$$T_e(d) = a[b^{1/2}(d) - 1], \tag{5}$$

with $a = 639$ K and

$$b(d) = 2.16 + 1723 \times P(1 - R)/d, \tag{6}$$

where P must be inserted in Watts and d in micrometers. Eq. (5) shows that the temperature T_e depends, at otherwise constant experimental parameters, solely on the spot diameter d . This dependence is shown in fig. 6 by the dashed curves which have been calculated from (5) for laser powers used in the deposition experiments (fig. 3).

(ii) With the 700 Å W/a-SiO₂ substrate, the situation is much more complicated. For short illumination times and/or low laser powers, the spot diameters observed are smaller than the laser focus and, as a consequence, in this regime the laser light is absorbed in part by the deposit and in part by the 700 Å sputtered W layer. Moreover, the thermal conductivities of the thin W

layer and of the quartz glass are not only quite different in magnitude but also have opposite temperature dependencies. Therefore, a solution of (1) can only be obtained numerically. Here, a finite-element method was employed. For the diameters d and the height h of spots, a ratio $d/h = 10$ has been assumed. The change in this ratio d/h , observed experimentally, has been shown to have only a very slight influence on the temperature T_ℓ [1,4]. The results of the calculations, i.e. the dependencies of the temperature T_ℓ on the W spot diameter, are given in fig. 6 by the full curves. In these calculations the temperature dependence of κ_D was also taken into account, i.e. the approximation (4) was *not* employed. The different curves shown correspond again to the laser powers at which the data presented in fig. 2 were obtained. Fig. 6 clearly demonstrates the great influence of the (thermally well-conducting) W layer on the temperature T_ℓ , and it also shows the extremely rapid change in this temperature with the laser-induced growth of the W spots.

5. Discussion

From a technological point of view, the experimental results demonstrate that for certain ranges of parameters, well-defined and smooth tungsten patterns of good morphology and height-to-diameter-ratios appropriate for many applications, for example in microelectronics, can be deposited. The smallest diameters of W spots produced on 700 Å W/a-SiO₂ substrates are, in the present experiments, around 0.6 μm. The increase in resolution over the 3 μm laser spot diameter is based on the nonlinearity of the deposition process and has been discussed in detail in ref. [1].

From a scientific point of view the preceding results permit an analysis of the fundamental mechanisms which dominate the deposition process. Additionally, such an analysis yields information on the kinetics of the growth process itself. This will be demonstrated in the following paragraphs.

The lateral growth rates of spots can be derived from figs. 2 and 3 by numerical differentiation, and are given by

$$W_\ell(\tilde{d}_i) = \frac{d_{i+1} - d_i}{2(t_{i+1} - t_i)}, \quad (7)$$

where $\tilde{d}_i = (d_{i+1} + d_i)/2$ is an average spot diameter derived from neighboring experimental data points $i+1$ and i taken at times t_{i+1} and t_i respectively. Clearly, in the regime of saturation, where $d_{i+1} \approx d_i$, this growth rate vanishes. If the growth of spots is a thermally activated process, the lateral growth rate within the kinetically controlled region can be described by an Arrhenius type law

$$W_\ell(\tilde{d}_i) = W_0 \exp(-\Delta E/R_G T_\ell(\tilde{d}_i)). \quad (8)$$

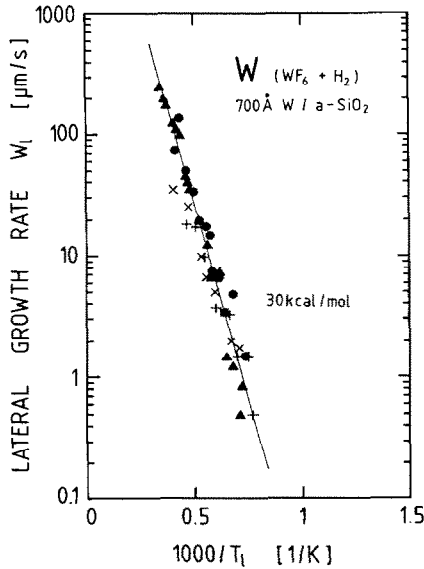


Fig. 7. Arrhenius plot for the lateral growth rate of W spots deposited with 647.1 nm Kr⁺ laser radiation from an admixture of 5 mbar WF₆ and 500 mbar H₂. The substrate was 700 Å W/a-SiO₂. The temperature T_l was calculated. The full line is a least-squares fit to all of the data points.

Here, $T_l(\tilde{d}_l)$ is the temperature at the edge of the spot, which can be calculated according to the procedure described in section 4; R_G is the gas constant, and ΔE the apparent chemical activation energy. It is evident that (8) cannot describe the regime of saturation observed experimentally and can therefore be employed only as long as $\tilde{d}_l < d_{max}$. Figs. 7 and 8 show Arrhenius plots for $W_l(\tilde{d}_l < d_{max})$ for the two substrate materials. The full line shown in fig. 7 is a least-squares fit to all of the data point. The full line in fig. 8 has been obtained correspondingly but only the data points within the low temperature regime, i.e. below the break in slope observed with higher temperatures, have been used for the fit. The figures show that within the accuracy of the measurements and of the overall analysis, data taken at different laser powers are fitted by approximately the same line. This demonstrates that the lateral growth rate of spots can in fact be described, in good approximation, by a thermally activated process. Within the regimes characterized by the full lines in figs. 7 and 8, this process is governed by the chemical kinetics. The apparent chemical activation energies derived from the figures are $\Delta E = 30 \pm 1$ kcal/mol and $\Delta E = 40 \pm 3$ kcal/mol for the 700 Å W/a-SiO₂ and the 1200 Å a-Si/a-SiO₂ substrate respectively. The somewhat wider scattering of data points in fig. 8 as compared to those in fig. 7 originates in part from the larger experimental inaccuracy obtained with a-Si/a-SiO₂ substrates and in part

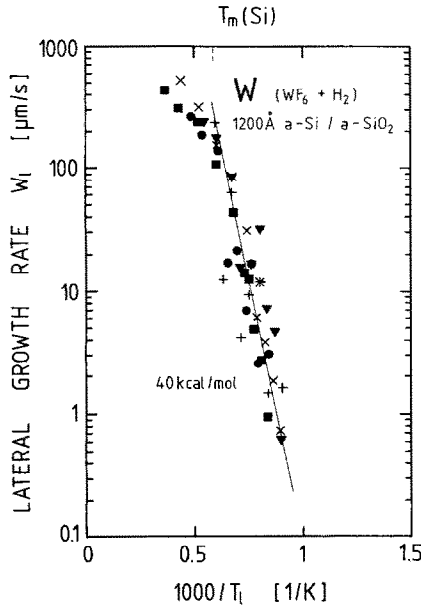


Fig. 8. Same as fig. 7 but for an 1200 Å a-Si/a-SiO₂ substrate. The full curve is a least-squares fit to data points at temperatures $T < T_m(\text{Si})$. T_m is the melting temperature of silicon.

from the uncertainties in the physical parameters of the a-Si entering the model calculations.

Further support for this analysis of the data is obtained by calculating the temperatures $T_\ell(d_{\max})$ that are related to the maximum diameters of spots obtained for the various laser powers (figs. 2 and 3). These temperatures are found to be *independent* of laser power and have values of $T_\ell(d_{\max}) = 1317 \pm 30$ K and $T_\ell(d_{\max}) = 1110 \pm 40$ K for the 700 Å W/a-SiO₂ and the 1200 Å a-Si/a-SiO₂ substrates, respectively. The consistency of the overall procedure can be demonstrated when the time evolution of spot diameters is calculated by integrating

$$\int_{d_s}^{d_i} d d' \exp\left(\frac{\Delta E}{R_G T_\ell(d')}\right) = \int_{t_s}^{t_i} dt, \quad (9)$$

where d_s and t_s are the starting points within a set of data obtained at a certain laser power, i.e. the d_s is the diameter of that spot which has been obtained with the shortest illumination time t_s . Clearly, the integral on the left-hand side of (9) must be calculated self-consistently because the temperature $T_\ell(d')$ depends on time via the spot diameter $d' = d'(t)$. The results of these calculations coincide for spot diameters up to $d \leq 0.8d_{\max}$ with the full curves shown in figs. 2 and 3. Note, however, that the spot diameters derived

from (9) increase continuously with laser beam irradiation time t_i . This is indicated in fig. 2 by the dashed curve which has been calculated for the 120 mW data. A phenomenological description of the saturation observed in the lateral growth of spots requires an extension of (8). This will be discussed below.

The power dependence of the spot diameter shown in fig. 4 can also be modelled with (9). The only difference is that we have to insert into (9) the power dependence of the temperature T_c , which can be calculated as described in section 4. The results of this calculation for the fixed illumination times $t_i = 0.5$ s and $t_i = 1$ s are given in fig. 4 by the full and dashed curves respectively. The quality of agreement between the experimental data and the calculated curves is another proof of the consistency of the description. It is interesting to note that the temperature that corresponds to the threshold power for deposition observed in fig. 4 is $T_{th} = 1985 \pm 30$ K. This temperature is considerably higher than the temperature $T_c(d_{max})$ at which the lateral growth of spots saturates. This difference in the temperatures derived can be qualitatively related to the nucleation process of W on 700 Å W/a-SiO₂ substrates. To start nucleation, a higher initial temperature is required.

We now will briefly discuss the values of activation energies derived from figs. 7 and 8. It has become evident that the type of substrate material not only influences the laser-induced temperature distribution, but also the chemical kinetics of the deposition process as well. In other words, the lateral growth kinetics is influenced by the physico-chemical properties of the substrate surface. This is quite different from the situation in standard CVD where, after the formation of some monolayers, the properties of the substrate become irrelevant.

The difference in the activation energy derived for the 700 Å W/a-SiO₂ substrate ($\Delta E = 30$ kcal/mol) and the activation energies derived from standard CVD of W (7.8–18 kcal/mol [13–15,19]) may indicate that the sputtered W layer, even when reduced in H₂ atmosphere prior to the laser-induced deposition, behaves differently from a growing virgin W layer. For example, if a thin oxide layer remains on the sputtered W film, it may considerably influence the various molecule–surface interactions involved in the deposition process. The analysis of standard CVD experiments has led to the (prevailing) interpretation that the rate-limiting mechanism in the overall reaction



is the dissociation of H₂ molecules adsorbed on the W surface. One may speculate that because of the different surface morphology and/or remaining surface oxides on the tungsten layers used in the present experiments, such a mechanism would require higher activation energies. There are, of course, many alternative possibilities that could explain the differences observed in activation energies. For example, as already discussed in ref. [1], homogeneous

gas-phase reactions may contribute substantially to the deposition process in standard CVD, while they are less important or even unimportant in laser CVD when the laser light is *not* absorbed within the gas phase, as is the case in the present experiments. An answer to some of these questions may be possible from investigations presently in progress into the axial growth of spots and the steady growth of rods.

The importance of molecule–substrate interactions also becomes evident in the experiments which use the 1200 Å a-Si/a-SiO₂ substrate. In this case, the a-Si layer directly participates in the surface reaction. This can be seen from a slight deepening of the substrate surface observed around the edges of W spots. A similar phenomenon has been observed before in connection with investigations on the direct writing of W stripes on a-Si/a-SiO₂ and crystalline Si substrates [3,7,16], and has been interpreted in terms of an initial reaction step, in which the WF₆ is directly reduced by the Si surface according to the overall reaction



This phase of silicon reduction is known to be self-terminating at a thickness of several hundred ångströms [17,18]. It is plausible that the tungsten layer formed according to (11) influences the lateral growth of spots in a different way to the sputtered W layer. However, the literature [17–22] appears to contain only little information about the activation energies involved in (11).

A final point in our discussion concerns the saturation observed in the lateral growth of spots. The origin of the related mechanism is not yet clear. There are, however, various different possibilities to qualitatively interpret this phenomenon: first of all, when the diameter of spots approaches the maximum diameter d_{max} , considerable changes in the morphology of the spots are observed. These changes are especially dramatic with high laser powers (fig. 1h). One may speculate that within this regime the effective value of R changes considerably so that the model calculations become inadequate. On the other hand, the calculations did yield, approximately the *same* temperature $T_\ell(d_{\text{max}})$ for *all* of the laser powers investigated for a certain substrate. This indicates that the quality of the model calculations is reasonable, at least up to temperatures $T_\ell(d \leq d_{\text{max}})$. Here, for the remainder of discussion, it is important to remember that the threshold temperature $T_\ell(d_{\text{max}})$ was found to be different with the two substrate materials. This may indicate that at low temperatures T_ℓ , i.e. in the regime of saturation, other surface mechanisms become important which, again, depend on the physico-chemical properties of the substrate material. Such mechanisms could be related to the surface diffusion of species, the dependence on surface coverage etc. Let us assume that for temperatures T_ℓ approaching $T_\ell(d_{\text{max}})$, the number of free adsorption sites, θ , at the edge of a growing spot becomes important in the reactions (10)

or (11). In this case, eq. (8) has to be modified and we can write it symbolically in the form

$$W_r(T(d_i)) = W_0\theta(T) \exp(-\Delta E/R_G T). \quad (12)$$

In the (dynamic) equilibrium, the flux of species adsorbed will be equal to the flux of species desorbed. This holds, of course, only as long as the net flux due to the surface reaction is negligible. If we assume that the energy of adsorption, ΔE_a , is small compared to the energy of desorption, ΔE_d , we obtain

$$\theta(T) = [1 + C \exp(\Delta E_d/R_G T)]^{-1}. \quad (13)$$

From the preceding discussion it is clear that $\theta(T)$ should have the following properties

$$\begin{aligned} \theta(T) &\rightarrow 1 && \text{with } T > T_\ell(d_{\max}) \text{ i.e. } d < d_{\max}, \\ \theta(T) &\rightarrow 0 && \text{with } T \approx T_\ell(d_{\max}) \text{ i.e. } d \approx d_{\max}. \end{aligned} \quad (14)$$

This can be achieved when the energy ΔE_d is very high. In fact, when using (12) instead of (8) in the integration (9), we can describe the lateral growth of spots within the *total* regime which includes the regime of saturation. The full curves in figs. 2 and 3 have been obtained in this way. Here, we have chosen for $\Delta E_d = 400$ kcal/mol, while C has been used as a fit parameter. This treatment permits a phenomenological description of the overall lateral growth of spots. It should be mentioned that the form of (12) and (13) is not specific to the mechanism discussed, but would also apply to other mechanisms, such as, for example, surface diffusion etc. On the other hand, the value of ΔE_d seems to be unrealistically high and the real microscopic process is probably much more complex. In fact, the sharp break in curvature observed when the temperature approaches $T_\ell(d_{\max})$, may also indicate a kinetic phase transition within the adsorbed layer [23].

6. Conclusion

Laser-induced chemical vapor deposition of W from mixtures of WF_6 and H_2 permits single-step patterning of substrates. The morphology of the W deposits can be controlled by the various different experimental parameters. With the experimental conditions investigated in the present paper, the deposition process can be described consistently on the basis of model calculations for *pyrolytic* LCVD. The growth kinetics derived in the present analysis depends significantly on the physico-chemical properties of the substrate material. Further insight into the microscopic mechanisms involved in the deposition process may be obtained from the pressure dependences of the growth rates.

Acknowledgement

We wish to thank Professor R. Chabicovsky for the sputtering of the W films and Professor U.M. Titulaer for a critical reading of the manuscript.

References

- [1] D. Bäuerle, *Chemical Processing with Lasers*, Vol. 1 of Springer Series in Materials Science (Springer, Berlin, 1986).
- [2] For recent reviews see:
 D. Bäuerle, Ed., in: *Laser Processing and Diagnostics*, Vol. 39 of Springer Series in Chemical Physics (Springer, Berlin, 1984) p. 166, and references therein;
 D. Bäuerle, K.L. Kompa and L.D. Laude, Eds., *Laser Processing and Diagnostics II* (Editions Physique, Les Ulis, 1986);
 A.W. Johnson, D.J. Ehrlich and H.R. Schlossberg, Eds., *Laser Controlled Chemical Processing of Surfaces* (North-Holland, New York, 1984);
 R.M. Osgood, S.R.J. Brueck and H.R. Schlossberg, Eds., *Laser Diagnostics and Photochemical Processing for Semiconductor Devices* (North-Holland, New York, 1983).
- [3] G.Q. Zhang, T. Szörényi and D. Bäuerle, *J. Appl. Phys.* 62 (1987) 673.
- [4] F. Petzoldt, K. Piglmayer, W. Kräuter and D. Bäuerle, *Appl. Phys. A* 35 (1984) 155.
- [5] K. Piglmayer and D. Bäuerle, in: *Laser Processing and Diagnostics II*, Eds. D. Bäuerle, K.L. Kompa and L.D. Laude (Editions Physique, Les Ulis, 1986) p. 79.
- [6] J. Doppelbauer and D. Bäuerle, in: *Interfaces under Laser Irradiation*, Eds., L.D. Laude, D. Bäuerle and M. Wautelet, *Nato ASI Series* (Nijhoff, Dordrecht, 1987) p. 277.
- [7] D. Bäuerle, *Spatial Inhomogeneities and Transient Behaviour in Chemical Kinetics* (Manchester University Press, Manchester, 1988).
- [8] R.C. Weast, Ed., *Handbook of Chemistry and Physics*, 59th ed. (CRC Press, Boca Raton, 1978/79).
- [9] Heraeus Inc., Germany: data sheet Q-A 1/112 (1979).
- [10] H.C. Webber, A.G. Cullis and N.G. Chew, *Appl. Phys. Letters* 43 (1983) 669.
- [11] S. Roberts, *Phys. Rev.* 114 (1959) 104.
- [12] H.S. Carslaw and J.C. Jaeger, *Conduction of Heat in Solids* (Oxford University Press, Oxford, 1959) p. 214.
- [13] W.A. Bryant, *J. Electrochem. Soc.* 125 (1978) 1534.
- [14] E.K. Broadbent and C.L. Ramiller, *J. Electrochem. Soc.* 131 (1984) 1427.
- [15] C.M. McConica and K. Krishnaman, *J. Electrochem. Soc.* 133 (1986) 2542.
- [16] G.Q. Zhang, T. Szörényi and D. Bäuerle, to be published.
- [17] C.M. Mellier-Smith, A.C. Adams, R.H. Kaiser and R.A. Kushner, *J. Electrochem. Soc.* 121 (1974) 298.
- [18] M.L. Green and R.A. Levy, *J. Electrochem. Soc.* 132 (1985) 1243.
- [19] C.-E. Morosanu and V. Soltuz, *Thin Solid Films* 52 (1978) 181.
- [20] J.-O. Carlsson and M. Boman, *J. Vacuum Sci. Technol. A* 3 (1985) 2298.
- [21] N. Lifshitz, *Appl. Phys. Letters* 51 (1987) 967.
- [22] H.J. Whitlow, T. Eriksson, M. Östling, C.S. Petersson, J. Keinonen and A. Anttila, *Appl. Phys. Letters* 50 (1987) 1497.
- [23] R.M. Ziff, E. Gulari and Y. Barshad, *Phys. Rev. Letters* 56 (1986) 2553.